Quiescent string dominance parameter F and classification of one-dimensional cellular automata

Sunao Sakai,* Megumi Kanno, and Yukari Saito
Faculty of Education, Yamagata University, Yamagata, Japan
(Received 28 March 2003; revised manuscript received 10 March 2004; published 4 June 2004)

The classification of rules may be one of the most fundamental targets in the study of cellular automata. In this paper, we propose a method for achieving such a classification, in which a new quiescent string dominance parameter F, which is orthogonal to λ, is introduced. For N-neighbor and K-state cellular automata, in the region $1/K<\lambda<1-1/K$, the maximum F corresponds to the class III rules, and its minimum, to the class II or class I rules. Therefore, transition of the pattern class takes place between them without fail. By using λ and F, the phase diagram of cellular automata is determined in the (λ,F) plane for five-neighbor and four-state cellular automata. The phase diagram indicates that along the F axis, class III rules are distributed in a large F region, while class I and class II rules are, in a small F region, and class IV rules are found in the overlapping region of class II and III rules. These distributions are almost independent of λ. Along the λ axis, all four pattern classes are found in the region $0.25<\lambda<0.75$, and no correlation between pattern class and λ parameter is observed.

DOI: 10.1103/PhysRevE.69.066117 PACS number(s): 89.75.−k

I. INTRODUCTION

Cellular automata (CA) are the mathematical models for complex systems. They consist of a lattice of sites, each of which takes a finite set of possible values (0 to $K-1$). The value of the site is called its state and it evolves synchronously in discrete time t according to a set of mappings which are defined by the N neighborhoods of the site around it. We denote such cellular automata as CA(N,K).

The states are represented as $s(t,i)$, where i is a position on the lattice. The time evolution of $s(t,i)$ is given by

$$s(t+1,i)=T\left[s\left(t,i-\frac{N-1}{2}\right),s\left(t,i-\frac{N-3}{2}\right),...,s(t,i),...,\right.$$
$$\left.\times s\left(t,i-\frac{N-3}{2}\right),s\left(t,i+\frac{N-1}{2}\right)\right]. \quad (1)$$

The set of mappings

$$T(\mu,\nu,...,\kappa,...,\rho,\sigma)=\eta,(\mu,\nu,\text{etc}.=0,...,K-1) \quad (2)$$

will be called the rule which consists of K^N entries. A set of states $s(t,i)$ at the same t is called a configuration, and a time sequence of the configuration forms a pattern.

It is well known that various patterns can be generated according to the chosen rules. Wolfram [1] classified these patterns into four rough categories: class I (homogeneous states), class II (simple separated periodic structures), class III (chaos aperiodic patterns), and class IV (edge of chaos; complex patterns of localized structure). The class IV patterns have been the most interesting target of studies of CA, because they provide us with examples of self-organization in a simple system, and it is argued that the possibility of computation is realized by the complexity at the edge of chaos [2,3].

Much more detailed studies of the patterns are carried out for elementary CA [CA(3,2)], in which patterns are studied by, computational mechanics [4], basin of attractor [5], etc. In this case however, the total number of independent rules is small enough (88) [6] that investigations of all of them have already been carried out, and their classification using some sets of parameters has also been studied [5–7].

Furthermore, for two-state CA, the symmetry of the interchange of states "0" and "1" seems to make the classifications of CA more delicate than those of CA with $K\geqslant 3$. Different results for the $\rho=1/2$ task in CA (7,2) have been obtained by Packard [8], and Mitchell, Crutchfield and Hraber [9]. Therefore, in order to elucidate general properties of the CA, it may be worth studying CA with $K\geqslant 3$.

However, if we proceed to the studies of general CA(N,K), the number of rules grows superexponentially K^{K^N}; therefore, except for a few CA(N,K) with small combinations of N and K, it is impossible to study all rules even within the lifetime of the universe. Therefore in order to classify these CA(N,K) rules, some other methods are necessary.

Studies in this direction have been started by Langton. He chose state "0" for quiescent states, and introduced the λ parameter as [3,10]

$$\lambda=\frac{N_h}{K^N}, \quad (3)$$

where N_h is the number of mappings in which η in Eq. (2) is not equal to 0. In other words, λ is the probability that the mappings do not select the quiescent state in the next time step. Langton claimed that as λ increases, the pattern class changes from class I to class II and then to class III, and that class IV behavior is observed between class II and class III pattern classes [3,10,11].

The λ parameter is thought to represent the average behavior of the CA rule space, but it ultimately does not sufficiently classify the quantitative behavior of CA. It is well

*Electronic address: sakai@e.yamagata-u.ac.jp

known that different pattern classes coexist at the same λ. Which of these pattern classes is chosen depends on the random numbers used in generating the rules. The reason or mechanism for this is not yet known; we have no way of controlling pattern classes at fixed λ. In Ref. [11], a schematic phase diagram was presented, however, a vertical axis was not specified. Therefore, it is indispensable to find a new parameter that will lead to a more quantitative understanding of the rule space of CA [12].

The purposes of this study are to find a new parameter F, which fixes the vertical axis of the phase diagram, and to obtain a phase diagram of CA in the (λ, F) plane. In this paper, we mainly focus on CA(5,4), because this is a model for which Langton has discussed the relationship between the λ parameter and pattern classes [3].

The outline of the paper is as follows. In Sec. II, we start by elucidating why different pattern classes are generated at the same λ. It is found that pattern classes have a strong correlation with the mappings that break strings of quiescent states. Then mappings are grouped into four types, according to the destruction and construction of strings of quiescent states. By introducing a method of changing the numbers of quiescent-string-breaking mappings, we can change pattern classes at will while keeping λ or N_h fixed. We also derive a theoretical explanation for why this change of pattern classes takes place without fail in the region $1/K \leqslant \lambda \leqslant 1-1/K$.

In Sec. III, the method of changing the pattern classes is studied quantitatively by introducing a new parameter, F, which we call the quiescent string dominance parameter. The maximum F corresponds to the class III pattern, and its minimum, to the class II or class I pattern. Therefore the transition of pattern classes is observed without fail somewhere between these maximum and minimum values.

The distribution of the rules in the (λ, F) plane is studied in Sec. IV. We generate about 14 000 rules randomly (details of the method are explained in a later section), and plot each of them on the (λ, F) plane. The distribution of the rules shows that throughout the range $1/4 \leqslant \lambda \leqslant 1-1/4$, all four pattern classes coexist. Class III rules are located in a large F region, while class II and I rules are, in a small F region, and class IV rules are found in their overlapping region. The correlation between the λ parameter and the pattern classes claimed by Langton [3] is not observed. We find that his result is dependent on the method of generating rules using probability λ.

In Sec. V, we determine the phase diagram (classification diagram of rule) of CA from the distributions of the class II and class III rules. It may be the first semiquantitative phase diagram which Langton sketched without fixing the vertical axis.

Section VI is devoted to discussions and conclusions. The transmission of initial-state informat ion, and other possible methods of determining the F parameter will be discussed.

II. STRUCTURE OF RULE AND PATTERN CLASSES

A. Correlation between pattern classes and quiescent-string-breaking mappings

In this paper, we fix the size of the lattice to be 150 and set a periodic boundary condition. A pattern is considered to fall into class IV when its transient length [3] is longer than 3000 time steps. The pattern class is discriminated by observing the pattern, the time sequence of spatial entropy $[H(t)]$ and the spatial probabilities of the states $[\rho^i(t), i=0,1,2,3]$. For a class II pattern, $H(t)$ and $\rho^i(t)$ converge to some fixed values or periodically repeat some fixed values, while for class III patterns, they fluctuate randomly. Typical pattern classes are shown in Figs. 1 and 2 [13].

First, we study whether or not the pattern classes are sensitive to initial configurations. We fix the rule and change initial configurations randomly. For most rules, details of the patterns depend on initial configuration, but the pattern classes are unchanged [1]. Thus differences in pattern classes are mostly due to those of rules, and the target of our inquiry concerns these differences between them.

For most rules, pattern class is determined by a randomly selected initial condition. However there are rules which generate different pattern classes depending on the initial configuration. These initial configuration dependences are observed for rules with long transient length. For these rules, about ten patterns are generated under random initial configurations and pattern classes are determined statistically. They will be further discussed in Sec. VI A, in connection with the transmission of initial-state information.

Up to Sec. III, we generate rules using only N_h, as follows. We start by choosing $1024-N_h$ mappings randomly and set $\eta=0$ on the right-hand side of Eq. (2). For the rest of the N_h mappings, η takes the value 1, 2, or 3 randomly.

For a short while, we do not impose the quiescent condition (QC), $T(0,0,0,0,0)=0$, because without this condition, the structure of the rule becomes more transparent. This point will be further discussed in Sec. III.

In order to elucidate why the different pattern classes are generated at the same λ, we collect rules of different pattern classes at the same λ, and look for differences between them. We set $N_h=450$ $(\lambda=0.44)$, because we empirically find that around this N_h point, class III, class II, and class IV patterns are generated in similar ratios. After some trial and error, we find a strong correlation between pattern classes and QC. We generate 20 rules for each of the class II, class III, and class IV patterns. Among them, the numbers of rules that satisfy QC are 20, 0, and 2 for class II, class III, and class IV patterns, respectively. This correlation suggests that the mapping $T(0,0,0,0,0)=h, h\neq 0$, which breaks a string of five quiescent states, pushes the pattern toward class III. We anticipate that a similar situation will hold for string of four quiescent states.

We return to the usual definitions of CA. In the following, we discuss CA under the QC, $T(0,0,0,0,0)=0$. The mappings which break the strings of four quiescent states are given by

$$T(0,0,0,0,i) = h,$$

$$T(i,0,0,0,0) = h, (i,h = 1,2,3). \tag{4}$$

We study the correlation between the number of these mappings and pattern classes.

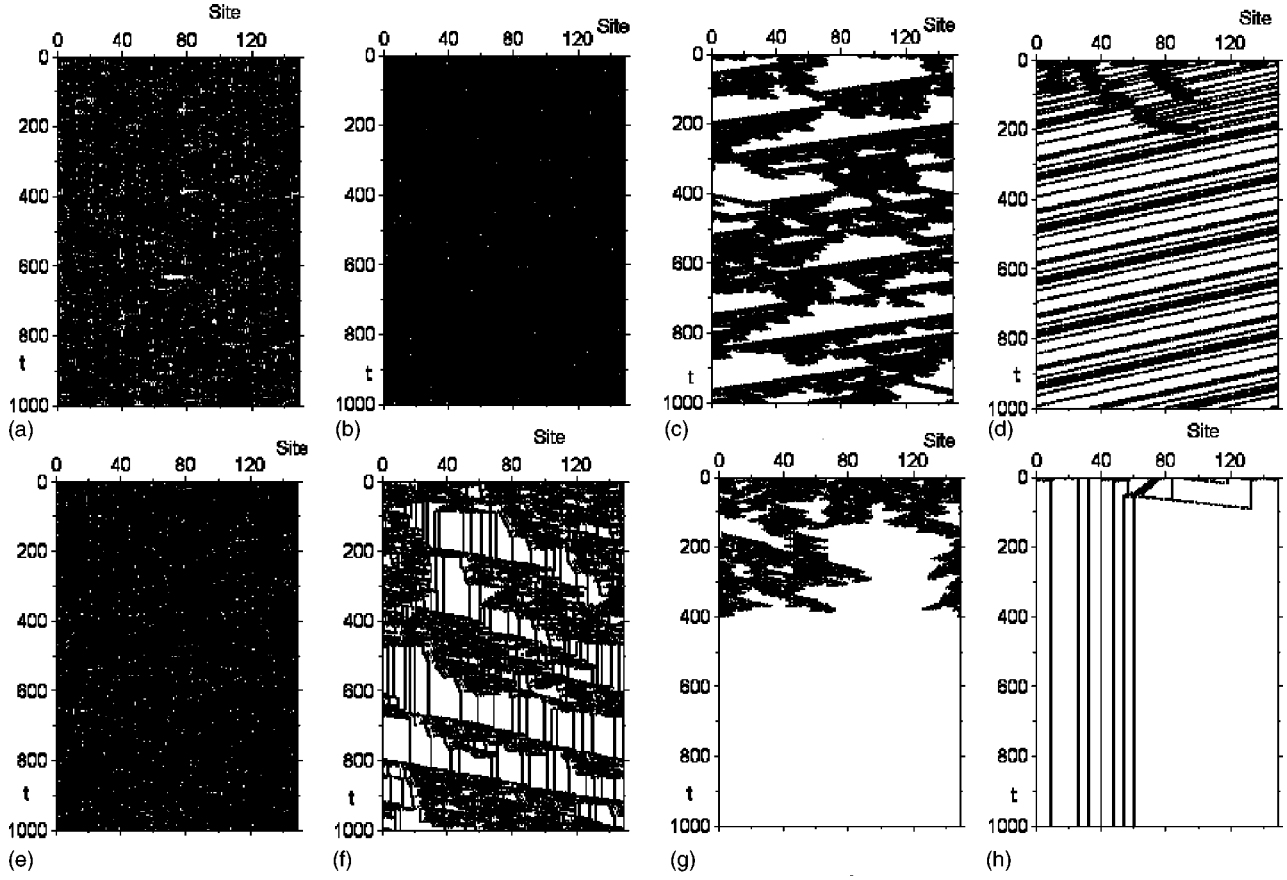

FIG. 1. Pattern classes at $N_h=450$. The quiescent state is shown by the white dot, while other states are indicated by black point: (a) $N_4=4$; (b), (c), (d) $N_4=3$; (e), (f), (g) $N_4=2$; (h) $N_4=1$.

We denote the total number of mappings expressed by Eq. (4) in a rule as N_4. In order to study the correlation between the pattern class and number N_4, we generate 30 rules and grouped them according to the number N_4. We have 4 rules with $N_4 \geqslant 4$, 13 rules with $N_4=3$, 9 rules with $N_4=2$, and 4 rules with $N_4 \leqslant 1$. When $N_4 \geqslant 4$, all rules generate class III patterns, whereas when $N_4 \leqslant 1$, only class II patterns are generated. At $N_4=3$ and $N_4=2$, class III, class II, and class IV patterns coexist. Examples are shown in Fig. 1. The coexistence of three pattern classes at $N_4=3$ is seen in Figs. 1(b)–1(d) and that of $N_4=2$ is exhibited in Figs. 1(e)–1(g).

As anticipated, strong correlation between N_4 and pattern class is also observed in this case. These discoveries have provided us with a key hint that leads us to the hypothesis that the mapping, which breaks strings of quiescent states, will play a major role in determining the pattern classes.

B. Structure of rule and replacement experiment

In order to test the hypothesis given in the preceding section, we classify the mappings into four groups according to their operation on strings of quiescent states. In the following, Greek characters in the mappings represent groups $0,1,2,3$ while Roman ones represent groups $1,2,3$.

Group 1: $T(\mu,\nu,0,\rho,\sigma)=h$.
The mappings in this group break strings of quiescent states.

Group 2: $T(\mu,\nu,0,\rho,\sigma)=0$.
The mappings in this group conserve strings.

Group 3: $T(\mu,\nu,i,\rho,\sigma)=0$.
The mappings in this group will develop strings of quiescent states.

Group 4: $T(\mu,\nu,i,\rho,\sigma)=l$.
The mappings in this group do not affect the string of quiescent states in the next time step.

Let us denote the number of group 1 mappings in a rule as $N(g1)$. The number of other groups is denoted similarly. These numbers $N(gi)$, $(i=1,2,3,4)$ satisfy the following sum rules, when N_h is fixed:

$$N(g1) + N(g2) = 256,$$

$$N(g3) + N(g4) = 768,$$

$$N(g2) + N(g3) = 1024 - N_h,$$

$$N(g1) + N(g4) = N_h. \tag{5}$$

In the methods of generating rules randomly using N_h or λ, these numbers are determined mainly by the probability λ; namely, $N(g1) \simeq 256\lambda$, $N(g2) \simeq 256(1-\lambda)$, $N(g3) \simeq 768(1-\lambda)$, and $N(g4) \simeq 768\lambda$. Therefore they suffer from fluctuation due to randomness.

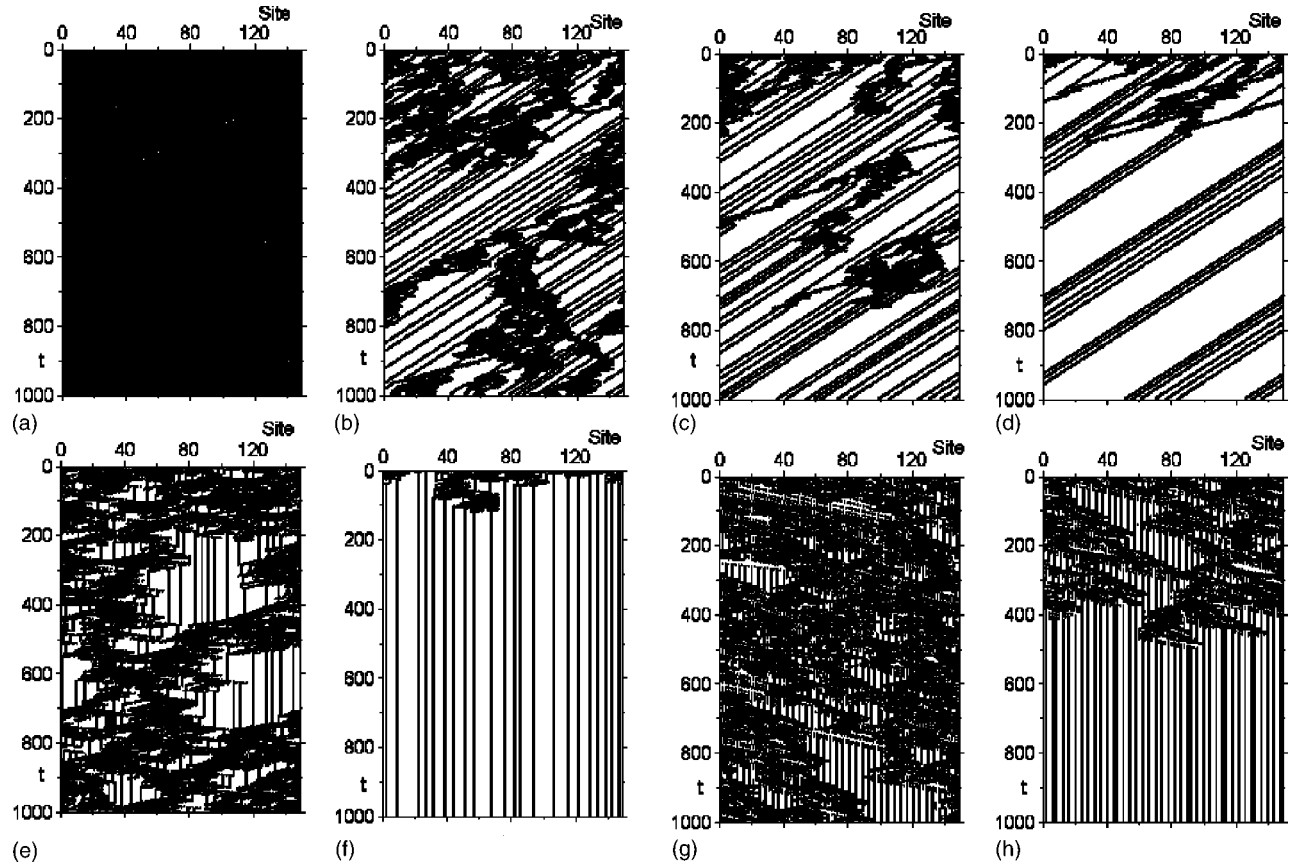

FIG. 2. Examples of the replacement experiments at $N_h=615$. (a) Obtained randomly with $N_h=615$, by the method explained in Sec. II A. (b) to (h) Obtained by the replacements of the rule of (a), which are summarized in Table II.

The group 1 mappings are further classified into five types according to the length of the string of quiescent states that they break. These are shown in Table I. Mapping D5 is always excluded from the rules by the QC. Our hypothesis presented at the end of Sec. II A is expressed more quantitatively as follows: the numbers of D4, D3, D2, and D1 mappings shown in Table I will mainly determine the pattern classes. In order to test this hypothesis, we artificially change the numbers of mappings in Table I while keeping N_h fixed. For D4 mappings, we carry out the replacements defined by

$$T(0,0,0,0,i)=h \rightarrow T(0,0,0,0,i)=0,$$

TABLE I. Classification of the mappings in group 1 into five types, where $h \neq 0$.

Type	Total number	Name	Replacement
$T(0,0,0,0,0)=h$	1	D5	RP5,RC5
$T(0,0,0,0,i)=h$	3	D4	RP4,RC4
$T(i,0,0,0,0)=h$	3		
$T(0,0,0,i,\sigma)=h$	12		
$T(i,0,0,0,m)=h$	9	D3	RP3,RC3
$T(\mu,j,0,0,0)=h$	12		
$T(\mu,j,0,0,m)=h$	36	D2	RP2,RC2
$T(i,0,0,l,\sigma)=h$	36		
$T(\mu,j,0,l,\sigma)=h$	144	D1	RP1,RC1

$$or\ T(i,0,0,0,0)=h \rightarrow T(i,0,0,0,0)=0,$$

$$T(\mu,\nu,j,\rho,\sigma)=0 \rightarrow T(\mu,\nu,j,\rho,\sigma)=l, \tag{6}$$

where, except for h, the groups μ, ν, ρ, σ, j, and l are selected randomly. Similarly, the replacements are generalized for D3, D2, and D1 mappings, and are denoted as RP4 to RP1 in Table I.

The reverse replacements for D4 are

$$T(0,0,0,0,i)=0 \rightarrow T(0,0,0,0,i)=h,$$

$$or\ T(i,0,0,0,0)=0 \rightarrow T(i,0,0,0,0)=h,$$

$$T(\mu,\nu,j,\rho,\sigma)=l \rightarrow T(\mu,\nu,j,\rho,\sigma)=0. \tag{7}$$

In this case, the group h, μ, ν, j, ρ, and σ are selected randomly. The replacements for D3, D2, and D1 are similarly defined, and are called RC4 to RC1.

With these replacements of RP4 to RP1 or RC4 to RC1, the numbers of mappings in Table I are changed, while N_h remains the same. We denote the numbers of D4, D3, D2, and D1 mappings as N_4, N_3, N_2, and N_1, respectively. We study whether or not these replacements change pattern classes. In these replacements, the RP4s are always carried out first, followed by RP3s. Examples are shown in Fig. 2.

TABLE II. The number of group 1 mappings and the number of replacements needed to obtain the pattern classes shown in Fig. 2

Figure	N_4	N_3	N_2	N_1	RP4	RP3	RP2	RP1
2(a)	3	22	53	96	0	0	0	0
2(b)	0	14	53	96	3	8	0	0
2(c)	0	13	53	96	3	9	0	0
2(d)	0	12	53	96	3	10	0	0
2(e)	1	7	53	96	2	15	0	0
2(f)	1	6	53	96	2	16	0	0
2(g)	2	1	53	96	1	21	0	0
2(h)	2	0	53	96	1	22	0	0

The rule of Fig. 2(a) is obtained randomly with $N_h=615$. At $N_h=615$, most of randomly obtained rules generate class III patterns. We first apply replacements RP4 three times, then N_4 becomes 0. At this stage, the rule still generates class III patterns. Then we proceed to carry out replacement RP3. The class III patterns continue from $N_3=22$ to $N_3=15$, and when N_3 becomes 14, the pattern changes to the class IV behavior, which is shown in Fig. 2(b). Figure 2(c) is obtained with one more RP3 replacement for the Fig. 2(b) rule. Figure 2(c) shows a class II behavior with a rather long transient length. The pattern with one more replacement of RP3 for Fig. 2(c) is shown in Fig. 2(d), where the transient length becomes shorter. In Table II, we have summarized N_4 and N_3, and the numbers of replacements RP4 and RP3 needed to obtain each rule in Fig. 2.

Similarly, experiments in which replacements RP4 are stopped at $N_4=1$ and $N_4=2$ are shown in Figs. 2(e)-2(f) and 2(g)-2(h), respectively. We note that the pattern changes from class III to class IV take place at ($N_4=0$, $N_3=13$), ($N_4=1$,$N_3=6$), and ($N_4=2$,$N_3=0$). Therefore the effect that pushes a rule toward class III is stronger for D4 than for D3. This point will be discussed more quantitatively in the following section.

At $N_h=819$, 768, 717, 615, 512, 410, 307, and 205, we carried out similar replacement experiments for 119, 90, 90, 117, 107, 92, 103, and 89 rules, respectively. At all N_h points, we succeeded in changing the pattern classes from class III to class II or class I, or vice versa, by these replacements. In many cases, class IV patterns were observed between them.

C. Chaotic and periodic limit of general CA(N,K)

Let us study the effects of the replacements theoretically in general CA(N,K). In the general case, rules are also classified into four groups, as shown in Sec. II B. We have denoted their numbers as $N(g1)$, $N(g2)$, $N(g3)$, and $N(g4)$. When N_h is fixed, these numbers satisfy the following sum rules, which are generalizations of Eq. (5).

$$N(g1)+N(g2)=K^{N-1},$$

$$N(g3)+N(g4)=K^{N-1}(K-1),$$

$$N(g2)+N(g3)=K^N-N_h,$$

TABLE III. Classification of CA(N,K) mappings into 4 groups. μ_i represents 0 to K-1 while h, i, and l represent 1 to K-1.

	Mapping type	Average number
Group 1	$T(\mu_1,\mu_2,\ldots,0,\ldots,\mu_N)=h$	$K^{N-1}\lambda$
Group 2	$T(\mu_1,\mu_2,\ldots,0,\ldots,\mu_N)=0$	$K^{N-1}(1-\lambda)$
Group 3	$T(\mu_1,\mu_2,\ldots,i,\ldots,\mu_N)=0$	$K^{N-1}(K-1)(1-\lambda)$
Group 4	$T(\mu_1,\mu_2,\ldots,i,\ldots,\mu_N)=l$	$K^{N-1}(K-1)\lambda$

$$N(g1)+N(g4)=N_h. \tag{8}$$

However, the individual number $N(gi)$ ($i=1,2,3,4$), suffers from fluctuations due to random number. The replacements needed to decrease the number of group 1 mappings while keeping N_h fixed are given by

$$N(g1)\rightarrow N(g1)-1,\quad N(g2)\rightarrow N(g2)+1,$$

$$N(g3)\rightarrow N(g3)-1,\quad N(g4)\rightarrow N(g4)+1. \tag{9}$$

These replacements stop either when $N(g1)=0$ or $N(g3)=0$ is reached (Table III). Therefore when $N(g1)\leqslant N(g3)$, which corresponds to $\lambda\leqslant(1-1/K)$ in λ, all group 1 mappings are replaced by group 2 mappings. In this limit, quiescent states at time t will never be changed, because there is no mapping which converts them to other states, while group 3 mappings have chances to create new quiescent states in the next time step. Therefore, the number of quiescent states in a configuration is a nondecreasing function of time t. Then, the pattern class should be class I or class II, which we call the periodic limit.

Let us discuss reverse replacements of Eq. (9). In these replacements, if $N(g2)\leqslant N(g4)$, which corresponds to $1/K\leqslant\lambda$, all group 2 mappings, except for the QC, are replaced by group 1 mappings. In this extreme reverse case, almost all quiescent states at time t are converted to other states in the next time step, while group 3 mappings create them at different places. Then the patterns will most probably develop into class III. This limit will be called the chaotic limit. We note that there is a possibility that atypical rules and initial conditions might generate periodic patterns even in this limit. However in this paper, these atypical cases are not discussed.

Therefore in the region $1/K\leqslant\lambda\leqslant 1-1/K$, all rules are located somewhere between these two limits, and by successive replacements of Eq. (9) and their reverse replacements, change of the pattern classes takes place without fail. This is the theoretical foundation for the replacement experiments described in the preceding section and also explains why four pattern classes coexist in this region.

The replacements defined by Eq. (9) and their reverse replacements, provide us with a method of controlling the pattern classes at the same N_h. The details of the replacements of Eq. (9) depend on the individual models. In the CA (5,4) case, these replacements were RP4 to RP1 and RC4 to RC1. By applying these replacements, we could study the rules, which are difficult to obtain using only N_h (or λ), and gain deeper understanding of the structure of CA rules space.

III. QUIESCENT STRING DOMINANCE PARAMETER *F* IN CA(5,4)

In the preceding section, we found that, in the region $1/K \leqslant \lambda \leqslant 1-1/K$, each rule is located somewhere between the chaotic limit and the periodic limit. In order to express the position of the rule quantitatively, we introduce a new parameter F which we call the quiescent string dominance parameter. It provides us with a new F axis orthogonal to λ. The minimum F is the periodic limit, while its maximum corresponds to the chaotic limit. In this section, we will determine the parameter F for CA(5,4).

As a first approximation, the parameter F is taken to be a function of the numbers of mappings D4, D3, D2, and D1, which have been denoted as N_4, N_3, N_2, and N_1, respectively. We proceed to determine $F(N_4,N_3,N_2,N_1)$ by applying simplest approximations and assumptions. We apply Maclaurin series expansion for F, and approximate it by the linear terms in N_4, N_3, N_2, and N_1.

$$F(N_4,N_3,N_2) \simeq c_4N_4 + c_3N_3 + c_2N_2 + c_1N_1. \tag{10}$$

Here, $c_4=\partial F/\partial N_4$, and similarly for c_3, c_2, and c_1. They represent the strength of the effects of mappings D4, D3, D2, and D1 that push the rule towards the chaotic limit. These definitions are symbolic, because numbers N_i are discrete. The measure in parameter F is still arbitrary. We set its unit such that an increase in one unit of N_4, results in a change of F by one unit. This corresponds to dividing F in Eq. (10) by c_4, and expressing it by ratios c_3/c_4 (r_3), c_2/c_4 (r_2), and $c_1/c_4(r_1)$.

Before we proceed to determine r_3, r_2, and r_1, let us interpret the parameter F geometrically. Most generally, the rules are classified in 1024-dimensional space, in case of CA (5,4). The location of the rule of each pattern class forms a hyperdomain in this space. We map these hyperdomains into those of four-dimensional (N_4,N_3,N_2,N_1) space. We introduce a hypersurface $S(N_4,N_3,N_2,N_1)=\Phi$ in order to align the points of class IV rules. In Eq. (10), we approximate it by a hyperplane. The F axis is the normal line to this plane.

Our strategy for determining r_3, r_2 and r_1 is to find the regression hyperplane of class IV rules on four-dimensional space (N_4,N_3,N_2,N_1). It is equivalent to fixing the F axis in such a way that the projection of the distribution of class IV rules on the F axis appears as narrow as possible. The quality of our approximations and assumptions reflects the width of the distribution of class IV rules. Using least squares, our problem is formulated to find r_3, r_2, and r_1 which minimize

$$s(r_3,r_2,r_2) = \frac{1}{c_4^2}\sum_{i,j}[F^i_{classIV}(N^i_4,N^i_3,N^i_2,N^i_1) - F^j_{classIV}(N^j_4,N^j_3,N^j_2,N^j_1)]^2, \tag{11}$$

where i and j indicate the class IV rules. We solve equations, $\partial S/\partial r_3=0$, $\partial S/\partial r_2=0$ and $\partial S/\partial r_1=0$, which are

TABLE IV. Optimal and intuitive coefficients r_i.

	Optimal	Error	Intuitive
r_3	0.1563	0.0013	0.18182
r_2	0.0506	0.0007	0.08333
r_1	0.0195	0.0002	0.04167

$$r_3\sum_{i,j}(\delta N_3^{i,j})^2 + r_2\sum_{i,j}\delta N_2^{i,j}\delta N_3^{i,j} + r_1\sum_{i,j}\delta N_1^{i,j}\delta N_3^{i,j} = -\sum_{i,j}\delta N_4^{i,j}\delta N_3^{i,j},$$

$$r_3\sum_{i,j}\delta N_3^{i,j}\delta N_2^{i,j} + r_2\sum_{i,j}(\delta N_2^{i,j})^2 + r_1\sum_{i,j}\delta N_1^{i,j}\delta N_2^{i,j} = -\sum_{i,j}\delta N_4^{i,j}\delta N_2^{i,j},$$

$$r_3\sum_{i,j}\delta N_3^{i,j}\delta N_1^{i,j} + r_2\sum_{i,j}\delta N_2^{i,j}\delta N_1^{i,j} + r_1\sum_{i,j}(\delta N_1^{i,j})^2 = -\sum_{i,j}\delta N_4^{i,j}\delta N_1^{i,j}, \tag{12}$$

where $\delta N_4^{i,j}=N_4^i-N_4^j$, and similarly for $\delta N_3^{i,j}$ and $\delta N_2^{i,j}$.

In order to collect class IV rules, we have generated rules randomly both for N_h in the region $205 \leqslant N_h \leqslant 819$ $(0.2 \leqslant \lambda \leqslant 0.8)$, and for numbers of group 1 mappings in the ranges $0 \leqslant N_4 \leqslant 6$, $0 \leqslant N_3 \leqslant 33$, $0 \leqslant N_2 \leqslant 72$, and $0 \leqslant N_1 \leqslant 144$.

This is realized by a two-step method. In the first step, we generate rules randomly according to the number N_h, as explained in Sec. II A. We note that at this step, the numbers of group 1 mappings, N_4, N_3, N_2, and N_1, are distributed around 6λ, 33λ, 72λ, and 144λ, respectively. They are denoted as N_i^λ. Then in the second step, each N_i is determined randomly between zero and its maximum. Each N_i^λ obtained in the first step is changed to the random value N_i by the replacements of RC4 to RC1 or RP4 to RP1.

We have generated about 14 000 rules, and classify them into four pattern classes. There are 483 class I, 3169 class II, 10248 class III, and 329 class IV rules, respectively. From the 329 class IV rules, the coefficients r_i are determined by solving Eq. (12). We call them optimal coefficients. The results are summarized in the column "optimal" of Table IV, where the statistical errors are estimated by the jackknife method. The result shows that coefficients are positive, and satisfy the order

$$c_4 > c_3 > c_2 > c_1. \tag{13}$$

This means that the effects that push rules toward the chaotic limit on the F axis are stronger for mappings which break longer strings of quiescent states.

If the quiescent condition is not imposed, Eq. (13) will become $c_5 > c_4 > c_3 > c_2 > c_1$. The correlation between pattern classes and D5 mapping will be stronger than that between D4 mappings. If we start our study under the QC, we

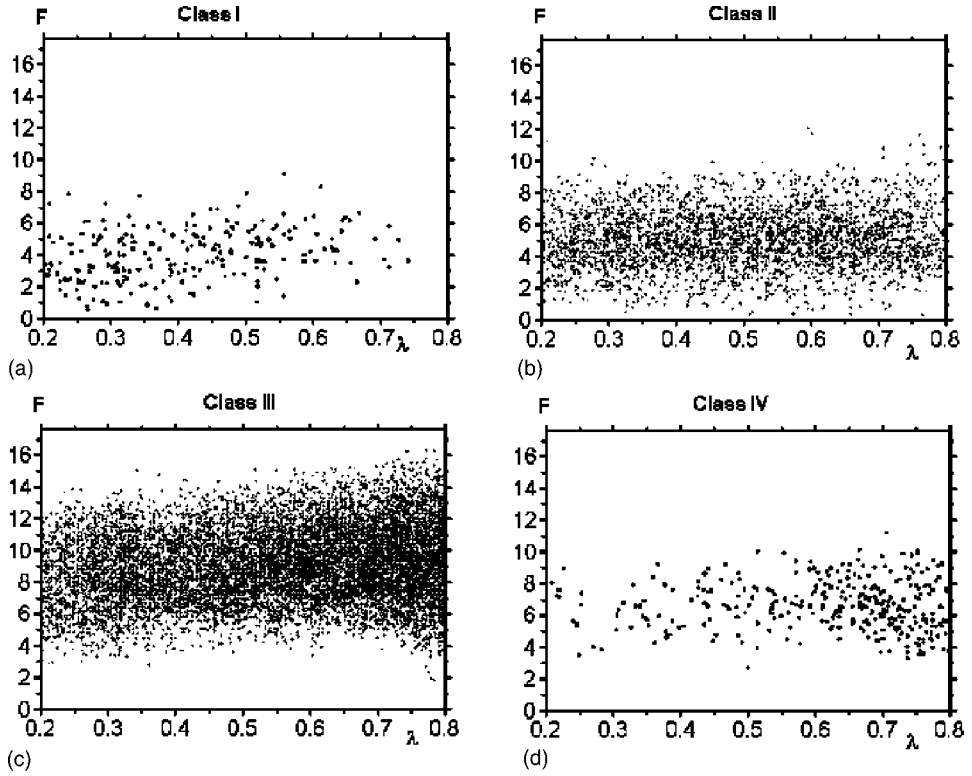

FIG. 3. Distribution of rules in (λ, F) plane. (a) Distribution of 483 class I rules. (b) Distribution of 3169 class II rules. (c) Distribution of 10248 class III rules. (d) Distribution of 329 class IV rules.

may make a longer detour to find the hypothesis and arrive at the qualitative conclusion presented in Sec. II.

The order in Eq. (13) is understood in terms of the following intuitive arguments. If six D4 mappings are included in the rule, the string of five quiescent states will not develop. Similarly, if 33 D3 mappings are present in the rule, there is no chance that strings of four quiescent states are made. These two situations are roughly similar for the formation of pattern classes. Thus the strength of the D3 mappings r_3 will be roughly equal to $6/33$ of that of D4 mappings; similar arguments apply for the strengths of the D2 and D1 mappings. We call these r_i intuitive coefficients, and they are also shown in the column "intuitive" of Table IV. It is found that differences between optimal and intuitive coefficients are not large. The classification of the rules with an intuitive F parameter will be discussed in Sec. VI B.

IV. DISTRIBUTION OF RULES IN (λ, F) PLANE

Using the optimal F parameter, we plot the position of each rule in the (λ, F) plane, as shown in Fig. 3. The class III rules are shown to be located in a large F region of about $F \geqslant 4$, while class I and class II rules are in a small F region of about $F \leqslant 9$, and class IV rules are found in the overlapping region of class II and class III rules of about $4 \leqslant F \leqslant 9$.

Figure 3 also reveals that at least in the $0.2 \leqslant \lambda \leqslant 0.75$ range, all four pattern classes coexist and that the classification of the CA pattern classes on the basis of the λ parameter is not confirmed, contrary to the results in Ref. [3]. Let us discuss the reason why Langton obtained his results. If rules are generated only by the probability λ using the "random-table method" or the "random-walk-through method" [3], numbers of group 1 rules N_4, N_3, N_2, and N_1 are also controlled by the probability λ. They are distributed around the N_i^{λ} as described in Sec. III. Then F parameters are also distributed around

$$F^{\lambda} = (6 + 33r_3 + 72r_2 + 144r_1)\lambda. \tag{14}$$

Therefore, in these methods, λ and F are strongly correlated. When λ is small, rules with small F are mainly generated, which are class I and class II CA. On the other hand, in the large λ region, rules with large F are predominantly generated, which are class III CA. The line F^{λ} of Eq. (14) crosses the location of class IV patterns at around $0.4 \leqslant \lambda \leqslant 0.55$. The probability of obtaining the rules that are far from the line given by Eq. (14) is very small. This might be the reason why Langton obtained his results.

The distribution of rules throughout the (λ, F) plane shows the global structure of the CA rule space, as in Fig. 3 and lead to a deeper understanding of CA.

V. CLASSIFICATION OF RULES IN (λ, F) PLANE

In Fig. 3, it is found that rules are not separated by sharp boundaries, but they have some probability distributions. We denote the probability densities of class I, class II, class III, and class IV rules as P^I, P^{II}, P^{III}, and P^{IV}, respectively and proceed to determine a phase diagram by using them.

The equilibrium points $F_E^{II\text{-}III}(\lambda)$ of class II and class III rules are defined by the point where the relation $P^{II}(F)$

TABLE V. The points N_h, numbers of each pattern class and the transition parameters of CA(5,4) .The column "Comp" shows the numbers of rules which transmit the information of initial states.

		Number of the rules					Class I-II			Class II-III		
λ	N_h	I	II	III	IV	Comp	$F_L^{I\text{-}II}$	$F_E^{I\text{-}II}$	$F_U^{I\text{-}II}$	$F_L^{II\text{-}III}$	$F_E^{II\text{-}III}$	$F_U^{II\text{-}III}$
0.125	128	202	1081	1052	42	16	0.0	2.0	3.2	3.0	6.6	9.0
0.15	154	99	499	545	23	17	0.7	2.0	3.6	3.5	6.5	9.1
0.2	205	141	728	1021	39	18	1.2	2.0	3.6	4.7	6.3	8.5
0.25	256	98	479	949	19	8	0.0	1.7	3.8	4.4	5.9	7.5
0.3	307	83	364	878	13	6	1.2	2.0	3.9	4.0	6.0	7.3
0.4	410	117	385	1169	23	7			3.7	4.5	5.7	7.0
0.5	512	53	341	884	23	7				4.8	6.0	7.2
0.6	615	38	488	1316	61	10				4.8	6.1	7.3
0.7	717	4	333	974	89	7				4.9	5.8	6.8
0.75	768	2	256	960	108	7				4.5	5.4	6.6
0.8	819	2	81	1064	12	5						4.3

$=P^{III}(F)$ is satisfied. The region where P^{II} and P^{III} coexist in a similar ratio defines the transition region. The upper points of the transition region $F_U^{II\text{-}III}$ are the points $P^{II}=P^{III}/e$, and similarly for lower points $F_L^{II\text{-}III}$, but P^{II} and P^{III} are interchanged. By using these three points, $F_E^{II\text{-}III}$, $F_U^{II\text{-}III}$, and $F_L^{II\text{-}III}$, we define the phase boundary of rules.

The distributions of the rules in Fig. 3 show the qualitative probability distributions. However, in order to study λ dependences of $F_E^{II\text{-}III}$, $F_U^{II\text{-}III}$, and $F_L^{II\text{-}III}$ more quantitatively, we generate rules independently at fixed N_h values. These N_h points and numbers of rules are shown in Table V. At each N_h point, we divide the region in F into sections of width $\delta F=1$, and count the number of rules of each class in these sections. From these numbers, we estimate the probability densities $P(F_i)$, where F_i is the midpoint of that section.

A. Classification of rules in $1/4 \leqslant \lambda \leqslant 1-1/4$

Let us proceed to the determination of the transition region of class II and class III rules. The probability distributions of $P^{II}(F)$ and $P^{III}(F)$ at $\lambda=0.3$ are shown in Fig. 4(a), and determinations of $F_E^{II\text{-}III}$, $F_U^{II\text{-}III}$, and $F_L^{II\text{-}III}$ are demonstrated in Fig. 4(b). For other λ points listed in Table V, the transition parameters $F_E^{II\text{-}III}$, $F_U^{II\text{-}III}$, and $F_L^{II\text{-}III}$ are determined in a similar manner. They are summarized in Table V. As already seen in Fig. 3, λ dependences of $F_E^{II\text{-}III}$, $F_U^{II\text{-}III}$, and $F_L^{II\text{-}III}$ are weak in the region $0.25 \leqslant \lambda \leqslant 0.75$. This is confirmed quantitatively by studies at the fixed λ values.

B. Classification of rules in large and small λ regions

P^{II} and P^{III} at $\lambda=0.8$ are shown in Fig. 5. It should be noted that there is no region of F where $P^{II} \geqslant P^{III}$. This means that $F_E^{II\text{-}III}$ and $F_L^{II\text{-}III}$ disappear. Only $F_U^{II\text{-}III}$ can be determined.

In order to understand what has changed at $\lambda=0.8$, we have studied the λ dependences of P^{II} and P^{III} in the region $\lambda \geqslant 0.7$, which are shown in Fig. 6. It is found that P^{III} gradually increases as λ becomes larger but the increase is quite small, while P^{II} decreases abruptly between $\lambda=0.75$ and $\lambda=0.8$. As a result, P^{II} becomes less than P^{III} in all F regions.

For the small λ region ($\lambda \leqslant 0.3$), behaviors of P^{II} and P^{III} are shown in Fig. 7. In this case, P^{II} gradually increases as λ decreases but the change is small. In contrast, the decrease in P^{III} is large. As a consequence of these changes, the transi-

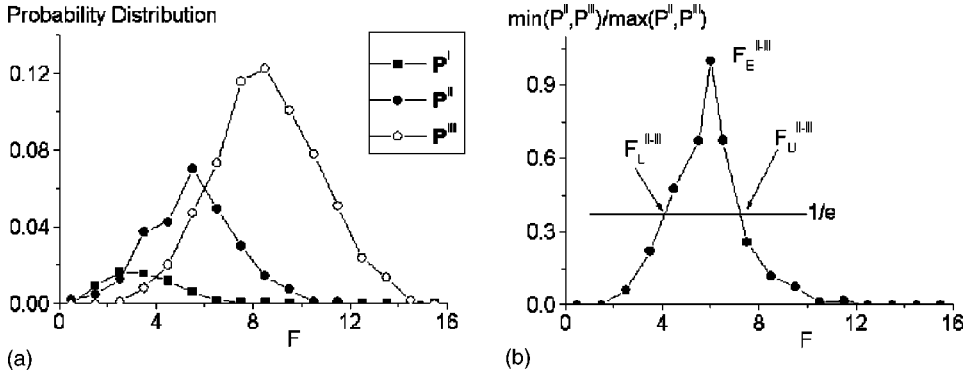

FIG. 4. Probability distributions P^I, P^{II}, and P^{III}, and determination of $F_E^{II\text{-}III}$, $F_L^{II\text{-}III}$, and $F_U^{II\text{-}III}$ at $\lambda=0.3$: (a) P^I, P^{II} and P^{III} distributions; (b) determinations of $F_E^{II\text{-}III}$ $F_L^{II\text{-}III}$, and $F_U^{II\text{-}III}$.

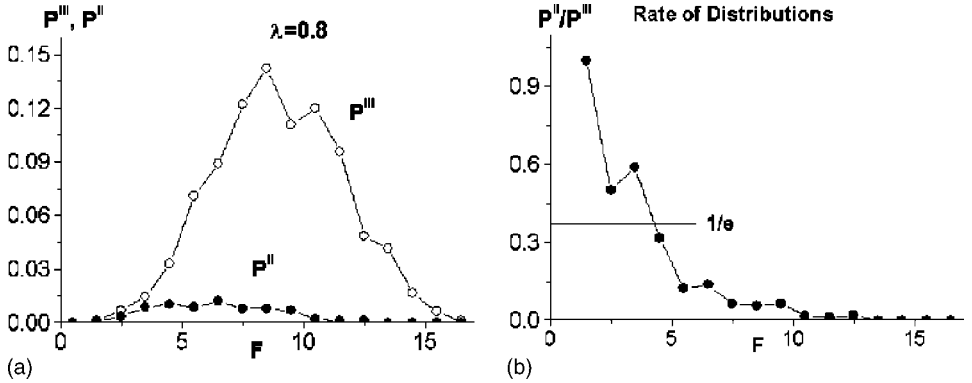

FIG. 5. Probability distributions P^{II} and P^{III} and the determination of $F_E^{II\text{-}III}$, $F_L^{II\text{-}III}$, and $F_U^{II\text{-}III}$ at $\lambda=0.8$: (a) P^{II} and P^{III}; (b) determination of $F_U^{II\text{-}III}$. P^{II} is larger than P^{III} in all regions of F, then $F_E^{II\text{-}III}$ and $F_L^{II\text{-}III}$could not be obtained.

tion region of class II and class III spreads over a wider range in F. These results are also summarized in Table V and shown in Fig. 8.

In the same way, the determination of the transition region of the class I and class II rules can be carried out. Preliminary results are shown in the columns of $F_E^{I\text{-}II}$, $F_U^{I\text{-}II}$, and $F_L^{I\text{-}II}$ of Table V. It is seen, in Figs. 3(a) and 3(b), that the density of class I rules decreases as λ increases, while that of class II rules stays almost constant in the region $\lambda \leqslant 0.75$. This feature is quantitatively confirmed by studies at the fixed λ values. At $\lambda=0.4$, the region of F where P^I is larger than P^{II} disappears, then $F_L^{I\text{-}II}$ and $F_E^{I\text{-}II}$ cannot be determined. This situation is similar to the P^{II} and P^{III} distributions at $\lambda=0.8$.

However, we would like to comment that neither the numbers of class I rules, nor those of the class II rules are not large in the region $F<3$, where the overlap region of class I and II CA will be located, therefore, the results may suffer from large statistical fluctuations. We believe that more data are required to achieve quantitative classification of class I and class II rules.

We proceed to classification of rules outside of these λ regions. In the $\lambda<0.25$ region, not all the group 2 mappings can be replaced by the group 1 mappings. Therefore, the maximum number of group 1 mappings $N(g1)_{Max}$ cannot become 256, and it decreases to zero as λ approaches to zero. Then the maximum $F(F_{Max})$, also decreases to zero toward $\lambda=0$. Conversely, in the $\lambda>0.75$ region, not all the group 1 mappings could be replaced by the group 2 mappings. The minimum $N(g1)$, and therefore the minimum $F(F_{Min})$, could not become 0. The line F_{Min} increases until its maximum at $\lambda=1$. In Fig. 8, we schematically show the F_{Max} and F_{Min} lines by dotted lines. We note that the dotted line should have some width due to fluctuations of N_4, N_3, N_2, and N_1 caused by randomness.

VI. DISCUSSIONS AND CONCLUSIONS

A. Transmission of initial-state information

Computability of CA is discussed very precisely, mainly for CA(3,2), in a series of papers [4]. In this section, we discuss the simplest problem of the transmission of initial-state information to later configurations.

We have found some examples of class II and class IV patterns appearing with similar probability upon changing initial configurations randomly. An example is shown in Fig. 9. It is also an example of the transmission of initial-state information to later configurations, similar to the $\rho=1/2$ problem in CA(N,2). These rules are found throughout the region of $0.125 \leqslant \lambda \leqslant 0.8$, and the numbers of rules with this property are also shown in the column "Comp" of Table V. It is interesting to investigate under what initial condition the changes of the pattern classes take place.

Although we focused on the differences of pattern classes between class II and class IV, because, in this case, differences between the patterns are obvious, there are cases where

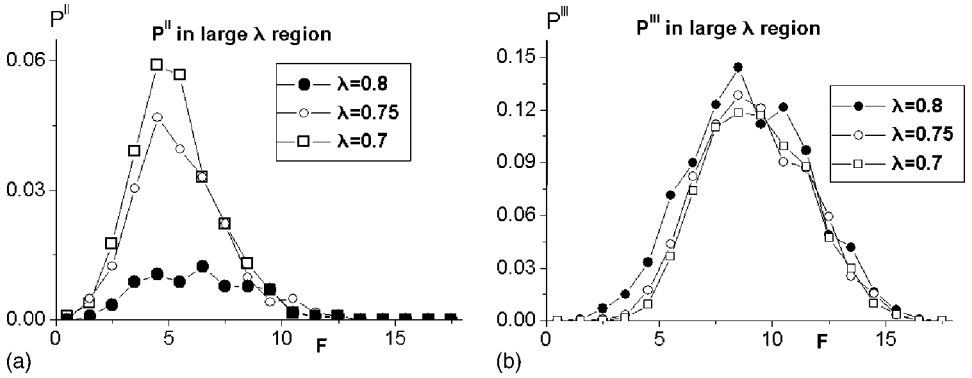

FIG. 6. λ dependences of P^{II} and P^{III} in the region $\lambda \geqslant 0.7$: (a) P^{II}; (b) P^{III}.

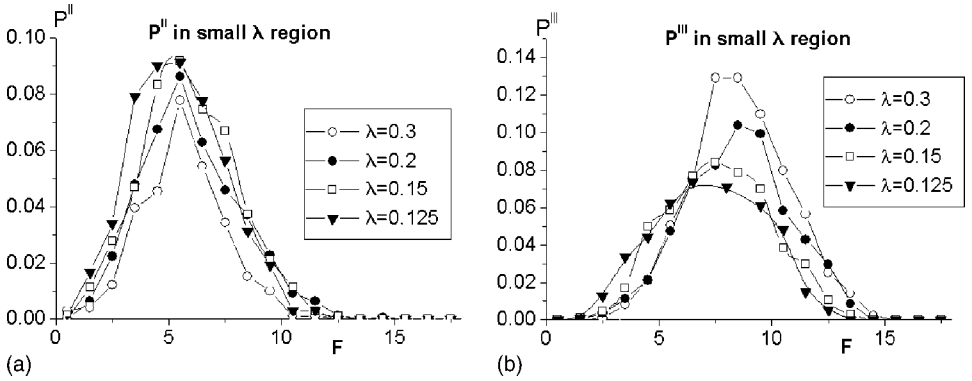

FIG. 7. λ dependences of P^{II} and P^{III} in the region $\lambda \leqslant 0.3$: (a) P^{II}; (b) P^{III}.

a difference between patterns is observed within the same pattern class. For example, different class II patterns are generated depending on initial configurations. These are also an example of the transmission of initial-state information.

B. Classification of rules by the intuitive *F* parameter

The methods of determining the coefficients r_i in Eq. (10) are not unique. In Sec. III, in order to determine them, we used the regression hyperplane of class IV rules, and in order to obtain 329 class IV rules, we generated a total of about 14 000 rules. This is a rather tedious task. However, the optimal set of r_i is close to the intuitive one.

We have studied the classification of rules using the intuitive F parameter. The same analysis as in Secs. IV and V are carried out using an intuitive set of coefficients. The results are very similar to Figs. 3 and 8, except that the scale of the vertical axis is enlarged; F_{Max} changes from 17.6 to 24 and the transition region in Fig. 8 shifts to about $6 < F < 11$.

If the intuitive F parameter could be used to successfully classify rules for general CA(N,K) it would be very convenient, because it is determined only by the structure of the CA rule and there would be no need to collect a large number of class IV rules. Whether it is successful or not must be concluded after studies of other CA(N,K) [14].

C. Conclusions

We began a search for the mechanism which distinguishes the pattern classes at the same λ, and found that the pattern classes are mainly controlled by the numbers of mappings that break strings of quiescent states (group 1 mappings).

In the region $1/K \leqslant \lambda \leqslant 1-(1/K)$, the maximum $N(g1)_{Max}$ corresponds to chaotic limit, and the minimum $N(g1)=0$, to periodic limit. Therefore in this λ region, we could always control the pattern classes using the replacements of Eq. (9) and their reverse replacements. Using these replacements, we could study the rules which are difficult to obtain only by N_h or λ. This property could be studied quantitatively by introducing the quiescent string dominance parameter F, and we found a method of obtaining a phase diagram.

In this study, the above procedure was applied for CA(5,4). In this case, the group 1 mappings were further classified into 5 types, as shown in Table I, and the classification of rules was carried out in the (λ,F) plane, as shown in Fig. 8. It was seen that λ dependences of the transition region are very gentle, and rules are classified better by the F parameter than by λ. It will be interesting to investigate whether the λ dependences of the transition region depend on CA(N,K) models.

In the replacement experiments, we observed class IV behavior in many cases. Examples are shown in Fig. 2. Sometimes they were observed in a rather wide range of the

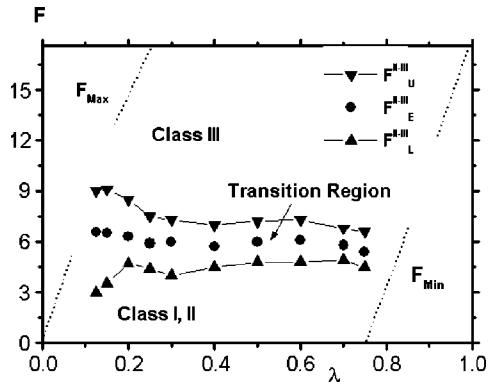

FIG. 8. Phase diagram of CA(5,4). The minimum of $F(F_{Min})$ and the maximum of $F(F_{Max})$, which are discussed at the end of Sec. V B, are schematically shown by the dotted lines.

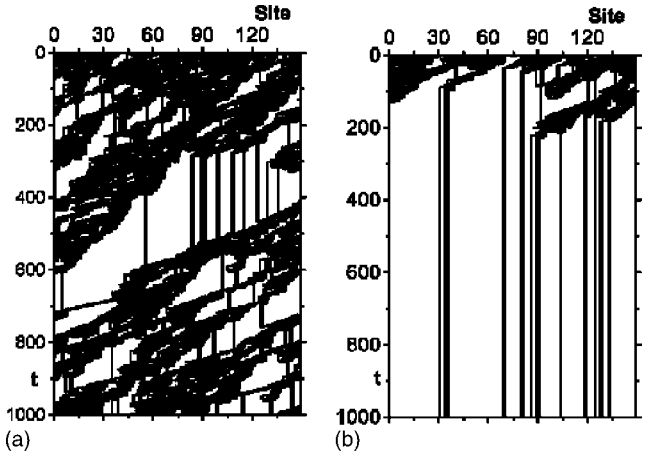

FIG. 9. An example of the transmission of initial-state information at $\lambda = 0.75$. (a) and (b) are generated by the same rule. The only difference is the initial-state configurations, which are set randomly.

replacements of N_3 or N_2. This indicates that in many cases, the transitions resemble second-order ones. However the widths in the ranges of N_3 or N_2 were different from each other, and there were cases where the width was less than one unit in the replacement of RP2; that is, it was first-order-like. It would be very interesting to investigate under what condition the transition becomes first-order-like or second-order-like. The mechanism of the difference in the transition is an open problem and it may be studied by taking into account the effects of group 3 and 4 mappings.

We note that in the transition region of Fig. 8, class II, III, and IV patterns coexist. The next step is to investigate the mechanism which distinguishes between them. In such studies, other new parameters will be found and a more quantitative phase diagram might be obtained. Our paper provides the next step in that direction.

These issues, together with finding the points where the transition region crosses F_{Max} and F_{Min} lines (dotted lines) in Fig. 8, and the nature of the transition at these points will be addressed in forthcoming publications.

[1] S. Wolfram, Physica D **10**, 1 (1984).
[2] S. Wolfram, Phys. Scr., T **T9**, 170 (1985).
[3] C. G. Langton, Physica D **42**, 12 (1990).
[4] J. E. Hanson and J. P. Crutchfield, Physica D **103**, 169 (1997), and references therein.
[5] A. Wuensche, Complexity **4**, 47 (1999).
[6] G. M. B. Oliveira, P. P. B. de Oliveira, and Nizam Omar, Artif. Life **7**, 277 (2001).
[7] P. M. Binder, Complex Syst. **7**, 241 (1993).
[8] N. H. Packard, in *Dynamic Patterns in Complex System*, edited by J. A. S. Kelso, A. J. Mandel, and M. F. Shlesinger (World Scientific, Singapore, 1988), pp. 293–301.
[9] M. Mitchell, J. P. Crutchfield, and P. T. Hraber, in *Proceedings of Santa Fe Institute Studies in the Science of Complexity*, edited by G. A. Cowan, D. Pines, and D. Meltzer (Addison-Wesley, Reading, MA, 1994), Vol. 19, pp. 497-513.
[10] C. G. Langton, Physica D **22**, 120 (1986).
[11] W. Li, N. H. Packard, and C. G. Langton, Physica D **45**, 77 (1990).
[12] In this paper, in accordance with Ref. [11], phase diagram and phase transition will be used in analogy with statistical physics.
[13] Strictly speaking, all patterns are periodic with 4^{150} time steps, because our spatial size is 150. However the period is very large, and we do not think that finite size effects will change our results.
[14] The preliminary studies on CA(5,3) and CA(5,5) indicate that the qualitative results are very similar to those of CA(5,4). The optimal set of the coefficients r_i of F are close to intuitive ones and the λ dependences of the transition region are very weak in the region $1/3 \leqslant \lambda \leqslant 2/3$ and $1/5 \leqslant \lambda \leqslant 4/5$ for CA(5,3) and CA(5,5), respectively and four pattern classes coexist there. The detailed studies on general CA(N,K) will be reported in the forthcoming publications.